3286–3292 *Nucleic Acids Research, 1998, Vol. 26, No. 13*

A mutation in *NPS1/STH1*, an essential gene encoding a component of a novel chromatin-remodeling complex RSC, alters the chromatin structure of *Saccharomyces cerevisiae* centromeres

Eiko Tsuchiya*, Tomoki Hosotani and Tokichi Miyakawa

Department of Fermentation Technology, Faculty of Engineering, Hiroshima University, Kagamiyama, Higashi-Hiroshima 739-8527, Japan

Received February 2, 1998; Revised and Accepted May 12, 1998

ABSTRACT

The *NPS1/STH1* gene encodes a nuclear protein essential for the progression of G2/M phase in *Saccharomyces cerevisiae*. Nps1p shares homology to Snf2/Swi2p, a subunit of a protein complex known as the SNF/SWI complex. Recently, Nps1p was found to be a component of a protein complex termed RSC (3) essential for mitotic growth, whereas its function is unknown. We isolated a temperature-sensitive mutant allele of *NPS1*, *nps1-105,* and found that the mutation increases the sensitivity to thiabendazole (TBZ). At the restrictive temperature, *nps1-105* arrested at the G2/M phase in *MAD1*-dependent manner and missegregated the mini-chromosome with higher frequency than the wild type cells. The nuclease digestion of the chromatin of the mutant cells revealed that the mutation causes the alteration of the chromatin structure around centromeres at the restrictive temperature. The results suggested that, in the *nps1-105* mutant, impaired chromatin structure surrounding centromeres may lead to an impairment of kinetochore function and the cells arrest at G2/M phase through the spindle-assembly checkpoint system.

INTRODUCTION

The DNA of eukaryotic genome is packed into chromatin basically consists of ~150 base pair (bp) DNA wrapped around an octamer of four histone proteins (H2A, H2B, H3 and H4). This nucleoprotein structure contributes to store huge DNA molecules within a nucleus but, at the same time, it confers a barrier for DNA metabolism, i.e., transcription, replication, repair or recombination.

Current studies on the regulation of eukaryotic gene expression revealed the presence of a protein complex, a SNF/SWI complex, which antagonizes chromatin-mediated repression of transcription (reviewed in 4–8). Purified yeast SNF/SWI complex contained at least 11 proteins (9–12). Biochemical analysis of the purified SNF/SWI complex revealed that this complex possesses a DNA-stimulated ATPase activity and can destabilize histone–DNA interactions in reconstituted nucleosomes in an ATP-dependent manner. The SNF/SWI complex is highly conserved through evolution: homologs of several Snf/Swi proteins have been identified in eukaryotes, and SNF/SWI complexes with related biochemical functions have been purified from human cells (13–16) and *Drosophila melanogaster* (17–19).

The Snf2/Swi2 subunit of the SNF/SWI complex contains a domain found in several DNA and RNA helicases and has been shown to harbor DNA-dependent ATPase activity (20). This protein is likely to play a key role in the chromatin remodeling activity of the complex. In *Saccharomyces cerevisiae*, a novel SNF/SWI-like complex termed RSC (remodel the structure of chromatin) was recently purified and characterized (3). RSC is an ~1 Mda complex that contains at least 15 polypeptides. The largest subunit of RSC that corresponds to Snf2/Swi2p of the SNF/SWI complex was proved to be the product of *NPS1/STH1* previously isolated by us and others (1,2). In addition to Nps1p/Sth1p, RSC contains at least three of which are related to components of the SNF/SWI complex: Rsc6p (related to Swp73p), Rsc8p (related to Swi3p) and Sfh1p (related to Snf5p) (3,21). Like the SNF/SWI complex, RSC showed a DNA-stimulated ATPase activity and was able to alter histone–DNA interactions in reconstituted mononucleosomes in an ATP-dependent manner (3). Despite the fact that the constituents of the SNF/SWI complex are encoded by non-essential genes, Nps1p/Sth1p, Rsc6p, Rsc8p and Sfh1p are encoded by genes essential for mitotic growth. Moreover, a LexA-Sth1p fusion protein did not activate transcription under conditions where an analogous LexA-Snf2 protein functions as a transcriptional activator (2), indicating that the RSC complex may play a wider role than the SNF/SWI complex. However, neither the physiological function nor the downstream targets of RSC have yet been identified. As we have previously reported, depletion of Nps1p arrests the cells at the G2/M phase (1). In addition, the recent finding that the temperature-sensitive sfh1-1 mutation also causes accumulation of cells with 2C-DNA content at restrictive temperature, indicates the requirement of RSC for the progression through G2/M phase (21).

To explore the function of Nps1p, we isolated a temperature-sensitive *nps1* mutant allele, *nps1-105*. In this report we describe the characterization of this mutant. We found that the *nps1-105*

*To whom correspondence should be addressed. Tel/Fax: +81 824 24 7868; Email: etsuchi@ipc.hiroshima-u.ac.jp

mutation causes the alteration of the chromatin structure on the centromeric DNA at the restrictive temperature. Our results provide a first clue in understanding the essential role of Nps1p and RSC in the cell division cycle.

MATERIALS AND METHODS

Media, yeast strains and manipulation

Both rich (YPD) and minimal (SD) media and basic yeast manipulations were as described (22). YP-galactose medium was prepared as for YPD, except that glucose (2%) was replaced by D-galactose (2%).

Experiments were performed in the yeast W303 (23) strain background (*ade2-1 leu2-3, 112 his3-11, 15 trp1-1 ura3-1*).

Generation of temperature-sensitive *NPS1* alleles

Hydroxylamine mutagenesis of pOS31*NPS1* (*NPS1*, *LEU2*, *CEN3*, *ARS1*) was carried out according to Rose *et al.* (22). We selected 6×10^3 transformants in WET-1D (*a*/α *nps1*Δ*::HIS3*/*nps1*Δ*::HIS3* YCp50*NPS1*) on SC-leucine plates and transferred to SC-leucine+5FOA plates. Colonies formed on SC-leucine+5FOA plates were screened for temperature sensitivity at 37 and 38°C by replica plating onto YPD plates. Plasmids were recovered in *Escherichia coli* and retransformed into WET-1D to confirm the temperature-sensitive phenotype. One plasmid pTH105-1 (*nps1-105*) which showed temperature sensitivity at 38°C was sequenced to identify the mutation.

The 5.8 kb *Xba*I fragment containing *nps1-105* was excised from pTH105-1 and transformed to WET-1 (*a nps1*Δ*::HIS3* YCp50*NPS1*) to replace the genomic *NPS1*-disruption allele (*nps1*Δ*::HIS3*) with the *nps1-105* mutant allele. Colonies grown on a SC+5FOA plate were checked for histidine auxotrophy and temperature sensitivity. Three candidate clones of the *nps1-105* mutant were transformed with pOS31*NPS1* to check for the suppression of temperature sensitivity and crossed to wild type strain to check for the segregation of the temperature-sensitive phenotype. The temperature-sensitive growth phenotype of all three clones was suppressed by the introduction of pOS31*NPS1* and the temperature-sensitive phenotype was segregated 2:2 in the progenies brought from all the crosses after sporulation. One of the temperature-sensitive progeny of these crosses was selected and named WTH-1 (*nps1-105*).

Plasmids, primers, plasmid constructions and strain constructions

The *MAD1* gene was cloned by PCR using primers A (ttttttagcg-gatccaagggtttac) and B (tagatcaatgttaaggtcgacccgt) with the genomic DNA as a template. The resulted fragment was cut with *Bam*HI and *Sal*I, and cloned into pUC119 (pUC*MAD1*). The *mad1*Δ*::TRP1* allele was created by replacing the internal *Bgl*II–*Sna*BI fragment of *MAD1* in pUC*MAD1* coding for amino acids 28–580 with the *Bam*HI–*Stu*I fragment of YRp7 containing the *TRP1* gene (pUC *mad1*Δ*::TRP1*). Plasmid pUC *mad1*Δ*::TRP1* was digested with *Sma*I and *Sal*I and introduced to W303-1A and WTH-1 to effect a one-step gene replacement of the chromosomal *MAD1* locus. The resultant strains were termed W-DM1 and WTH-DM1, respectively.

Flow cytometry

Flow cytometry analysis was performed on a Coulter Epics Elite ESP. Cells were prepared as described previously (1). Each FACS scan was performed on 2×10^4 cells.

Digestion of chromatin with nucleases and Southern blot

Cells of W303D (*a*/α) and WTH-1D (*a*/α *nps1-105/nps105*) in mid-log phase were rapidly shifted from 27 to 38°C by the addition of an equal volume of medium pre-warmed to 45°C. After 3 h incubation, cells were harvested and converted to sphearoplasts as described by Szent-Gyorgyi and Isenberg (24) with the following modifications. Sodium azide and phenylmethylsulfonyl fluoride (PMSF) were added to 20 and 0.5 mM, respectively, immediately prior to harvesting the cells. Zymolyase 100T (Seikagaku Kogyo, 50 µg/ml) was used instead of lyticase. Sphearoplasting was carried out for 30 min at 34 or 38°C for the cells without or with the heat treatment, respectively. Sphearoplast suspensions were then diluted with 4 vol of buffer A (1.4 M sorbitol, 40 mM N-2-hydroxyethylpiperazine-N′-2 ethanesulfomic acid/KOH, pH 7.5, 0.5 mM $MgCl_2$, 20 mM NaN_3, 0.5 mM PMSF) and sphearoplast concentration was estimated by measuring the optical density of the suspension at 260 nm after the lysis in 1% sodium dodecyl sulfate. Sphearoplasts corresponding to OD_{260} value of 150–250 were harvested by centrifugation, washed once with buffer B [1 M sorbitol, 10 mM piperazine-N, N-bis 2-ethanesulfonic acid (PIPES), pH 7.5, 0.2 mM $CaCl_2$, 20 mM NaN_3, 0.5 mM PMSF] and resuspended in 2 ml of MNase digestion buffer (10 mM PIPES, pH 7.5, 0.2 mM $CaCl_2$, 1 mM PMSF, 20 mM NaN_3) or *Dra*I digestion buffer (10 mM Tris–HCl, pH 7.5, 10 mM $MgCl_2$, 50 mM NaCl, 1 mM dithioerythritol, 1 mM PMSF, 20 mM NaN_3) (25). The suspension was prewarmed at 37°C for 2 min, and MNase (50 U/ml, Boehringer Mannheim) was added. Samples were withdrawn at various time points and EDTA was added to 25 mM to stop reaction. For *Dra*I digestion, various amounts of *Dra*I were added to each sphearoplast suspension (300 µl) and the reaction was carried out at 37°C for 30 min. After the digestion, DNA was deproteinized and purified as described by Ling *et al.* (26). For the experiments with naked DNA, sphearoplasts were prepared exactly as described for chromatin digests, but immediately before nuclease cleavage, DNA was deproteinized and purified. Southern blot analysis was done by using fluorescein-labeled probes and Gene Images labeling and detection kit (Amersham). Probes used for detecting *CEN3* and *CEN4* are the 592 bp *Nhe*I–*Bam*HI fragment from pOS31 that contains *CEN3* DNA sequence and the 1018 bp *Spe*I–*Stu*I fragment from YCp50 that contains *CEN4* DNA sequence, respectively.

Analysis of DNA topoisomers

The topoisomer distribution of the yeast 2 µm circle plasmid DNA was assayed as described previously (27). Topoisomers were separated by electrophoresis in 1% agarose gels containing 2.5 µg/ml of chloroquine and detected by Southern blot as described in the above section. The *Eco*RI–*Sna*BI fragment from YEp24 that contains the 2 µm DNA sequence was used to probe endogenous 2 µm plasmids.

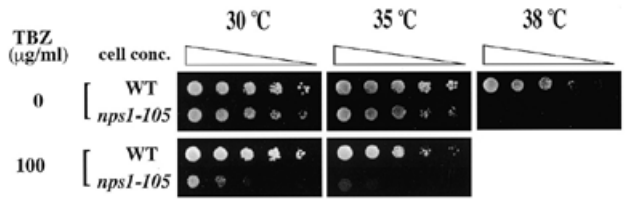

Figure 1. Phenotypes of *nps1-105*. Wild type and *nps1-105* were grown to mid-log phase and spotted on YPD plates or YPD plates containing 100 μg/ml of TBZ and incubated at the indicated temperatures for 3 days.

Mini-chromosome missegregation assay

The mitotic segregation of *SUP11* marked mini-chromosomes (pHM410, *SUP11*, *URA3*, *CEN4*, *ARS1*) in the strains YTW-30D (*a*/α *ade2-101/ade2-101*) and YTW-n9D (*a*/α *ade2-101/ade2-101 nps1-105/nps1-105*) was monitored using the color colony assay (28). In each assay, three mostly pink colonies were picked from color media plates and used for the experiment. Cells were grown to mid-log phase at 27°C and shifted to 38°C (experiment 1) or added TBZ to 60 μg/ml and then shifted to 34°C (experiment 2). After each treatment (3 h), ~100 cells were spread on color media plates after a brief sonication (5 s). These plates were incubated for 5 days at 25°C and then overnight at 4°C. Three independent assays were performed to monitor the segregation of pHM410.

RESULTS

Isolation of a *NPS1* temperature-sensitive mutant

In order to investigate the role of *NPS1*, we generated conditional *NPS1* alleles by employing hydroxylamine-directed *in vitro* mutagenesis. Mutagenized plasmids were introduced into *NPS1* deletion strain carrying wild type *NPS1* on a plasmid by plasmid shuffling. One plasmid that allowed growth at 30 but not at 38°C was chosen for further analysis. The mutant allele was designated as *nps1-105*. This allele was replaced with the genomic *NPS1* locus of WET-1 (*nps1*Δ::*HIS3*) by one step gene replacement to make the *nps1-105* mutant strain (Materials and Methods). Upon shift to 38°C, the *nps1-105* mutant stopped growth with an accumulation of large-budded cells possessing a single nucleus of a 2C-DNA content (Fig. 2, data for cellular and nuclear morphologies are not shown). These phenotypes were consistent with that of the cells carrying galactose-inducible *NPS1* after shifting to glucose medium (1). DNA sequence determination revealed that *nps1-105* carries a single base substitution within the open reading frame (ORF): G to A at position 2288 resulted in the amino acid substitution of cysteine to tyrosine at position 763. The Cys763 of Nps1p is conserved in Snf2p but not located within or near the conserved helicase sequence motif. In case of Nps1p, this amino acid residue exists near the essential Lys792 (1) which may serve as the ATP binding site in association with G-rich motif 20 amino acids upstream of Cys763.

nps1-105 shows increased sensitivity to microtubule-destabilizing agents

In addition to temperature-sensitive growth phenotype, the *nps1-105* mutant showed increased sensitivity to microtubule-destabilizing agents such as thiabendazole (TBZ), methylbenzcarbamate (MBC) and benomyl (Fig. 1, data for MBC and benomyl are not shown). The *nps1-105* mutant could not grow on a YPD plate containing >110 or 70 μg/ml of TBZ at permissive (<30°C) or at semipermissive temperature (35°C), respectively. The wild type strain, on the other hand, could grow on a YPD plate containing up to 160 μg/ml of TBZ at both 30 and 35°C.

We also tested the sensitivity of *nps1-105* to hydroxyurea, methylmethane sulphonate, cycloheximide and trifluoperazine. No difference was observed between wild type and *nps1-105* in the sensitivity to these drugs, indicating that the mutant is specifically sensitive to microtubule-destabilizing agents (data not shown). Both temperature and TBZ sensitivities of *nps1-105* cosegregated in the haploid progenies from *NPS1*/*nps1-105* diploid after sporulation, and complemented by the introduction of wild type *NPS1* on a low-copy-number plasmid (data not shown).

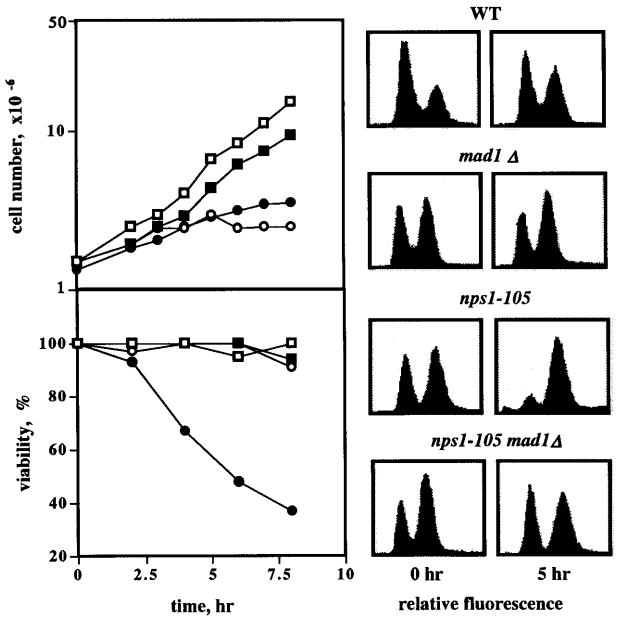

Figure 2. The cell cycle arrest of *nps1-105* at the restrictive temperature depends on *MAD1*. (**A**) Growth and viability of *nps1-105* and *nps1-105 mad1*Δ mutants. Wild type (W303-1A, open square), *mad1*Δ (W-DM1, closed square), *nps1-105* (WTH-1, open circle) and *nps1-105 mad1*Δ (WTH-DM1, closed circle) cells were grown to early-log phase at 25°C and shifted to 38°C. At the times indicated in the figure, cell counts were obtained, diluted to appropriate numbers and plated on YPD medium at 25°C. Viability is presented as the percentage of cells that could form colonies at 25°C. Values are the average of three independent determinations; standard deviations were within 30%. (**B**) Flow-cytometric analysis of the DNA content of *nps1-105* and *nps1-105 mad1*Δ cells. Cultures analyzed in (A) were stained with propidium iodide and analyzed for DNA content using a flow cytometer. Results are plotted as the relative amount of DNA per cell versus the number of cells.

MAD1 disruption causes a failure in the cell cycle arrest and loss of viability in *nps1-105* at the restrictive temperature

The above observations indicated the possibility that *NPS1* affects the organization and/or stability of mitotic spindles. Spindle malformation is detected by spindle-assembly checkpoint control including *MAD* and *BUB* gene products as components (reviewed in 29). If Nps1p is involved in these processes, the cell cycle arrest of *nps1-105* at elevated temperature is interfered with by the loss of spindle-assembly checkpoint function. To test this

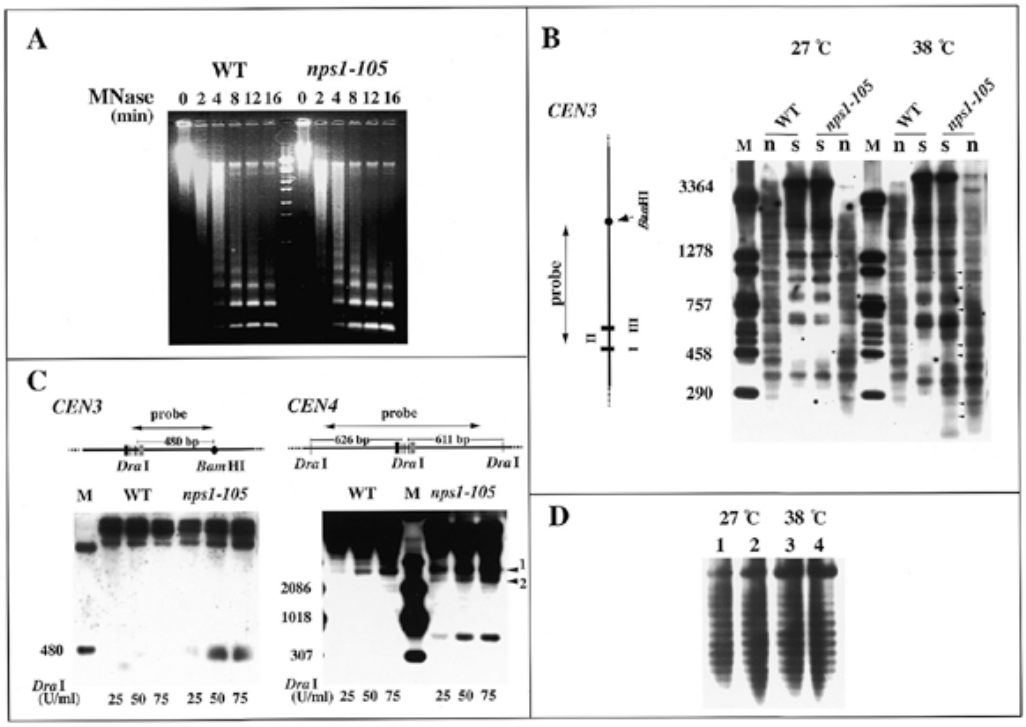

Figure 3. Effects of the *nps1-105* mutation on chromatin structures. (**A**) MNase digestion pattern of the wild type and the *nps1-105* chromatin. Wild type (WT) and *nps1-105* cells were grown to mid-log phase at 27°C, shifted to 38°C for 3 h and converted to sphearoplasts. Sphearoplasts (125 OD_{260} U/ml) were digested with 50 U/ml of MNase at 37°C for the times indicated and DNA was deproteinized and purified. DNA samples were subjected to electrophoresis on 1.3% agarose gel and stained with ethidium-bromide. (**B**) MNase-sensitive sites on the centromeric chromatin from chromosome III. Sphearoplasts (75 OD_{260} U/ml) prepared as described in (A) were digested with 50 U/ml of MNase for 80 s at 37°C (lanes s). MNase digestion of naked DNA (lanes n) was carried out with 1 U/ml of MNase for 50 s at 37°C. After deproteinization and purification, DNA samples were subsequently digested with *Bam*HI and subjected to Southern blot analysis with fluorescein labeled *Nhe*I–*Bam*HI fragment of *CEN3*. The sizes of molecular weight markers (M) are indicated in bp. At the left side of (B), schematic map of the chromosome region surrounding *CEN3* is cited. *Bam*HI cleavage site is indicated with a closed circle. I, II and III show the relative position of the sequence elements CDEI, CDEII and CDEIII, respectively. (**C**) *Dra*I accessibility of *CEN3* and *CEN4* chromatin increases in *nps1-105* upon shift to 38°C. Sphearoplasts (90 OD_{260} U/ml) were prepared from wild type and *nps1-105* cells treated for 3 h at 38°C and digested with *Dra*I for 30 min at 37°C. Genomic map of DNA regions surrounding *CEN3* and *CEN4* is schematically indicated at the top of the panel with the positions of probes used for Southern hybridization. Relative positions of CDEI and CDEIII are denoted by black and shadowed boxes, respectively, and CDEII lies between these elements. *Dra*I and *Bam*HI sites are indicated with bars and a closed circle, respectively. Arrowheads 1 and 2 at the right side of *CEN4* panel indicate 2400 and 2100 bp fragments, respectively. The sizes of molecular weight markers (M) are indicated in bp. (**D**) Superhelicity of endogenous 2 µ plasmid DNA in wild type and *nps1-105* cells. Wild type (lanes 1 and 3) and *nps1-105* (lanes 2 and 4) cells were grown at 27°C to early-log phase and treated at 38°C for 3 h. DNA samples prepared from the cells without (lanes 1 and 2) and with the heat treatment (lanes 3 and 4) were separated on agarose gels containing 2.5 µg/ml of chloroquine and subjected to Southern blot analysis.

possibility, we disrupted the *MAD1* gene in the *nps1-105* mutant. The *nps1-105 mad1*Δ double mutant could not arrest at G2/M phase after 5 h incubation at 38°C (Fig. 2). In addition, viability of the double mutant cells decreased in dependence with the incubation period at 38°C. In contrast, no notable decrease of viability was observed with wild type, *nps1-105* or *mad1*Δ mutants in 8 h incubation at 38°C.

The *nps1-105* mutation alters the chromatin structure around the centromere

Recent finding that RSC exhibits an activity to perturb nucleosome structure *in vitro* (3) and our results described above, suggested the possibility of the relevance of Nps1p on the chromatin structure at centromeres. Bloom and Carbon showed that yeast centromeres are packaged into a unique chromatin structure composed of a nuclease-resistant core flanked by ordered arrays of nucleosomes (30). We examined the chromatin structure of *CEN3* and flanking sequences in *nps1-105* after 3 h incubation at 38°C. Permeabilized sphearoplasts were partially digested with micrococcal nuclease (MNase) and DNA was deproteinized and digested with *Bam*HI. Southern blot analysis of the DNA sample from the wild type cells with *CEN3* probe showed that a 250 bp centromere-core region of DNA occurring between 350 and 600 bp from *Bam*HI recognition site was protected from MNase digestion (Fig. 3B). In the region flanking *CEN3* core region, an extensive series of MNase cutting sites were seen at ~160 bp intervals as described by Bloom and Carbon (30). In the wild type strain, this cutting pattern was not altered after the 3 h incubation at 38°C. The cutting pattern of the DNA sample from *nps1-105* cells grown at 27° was indistinguishable from that of wild type, while a number of faint cutting sites not seen in the wild type chromatin lanes appeared within the centromere core and in the flanking region in the *nps1-105* incubated at 38°C lanes (indicated with arrowheads). As demonstrated in Figure 3A, overall MNase cutting pattern of chromatin of the 38°C-treated wild type and mutant cells showed no change, indicating that the increase in nuclease accessibility of heat-treated *nps1-105* chromatin is specific to the region around *CEN3*.

Next, we asked if the structural changes of chromatin occur in other centromere regions. The perturbation in the structural integrity of centromere DNA could be examined by the increase in nuclease accessibility of chromatin for restriction enzyme sites within the internal centromere region. *Saccharomyces cerevisiae* centromere DNA contains three elements, CDEI, CDEII and CDEIII (31–33). CDEI and CDEIII are 8 and 25 bp DNA elements with partial dyad symmetry, respectively. CDEII is a 76–86 bp region highly rich in A and T and contains at least one *Dra*I recognition site (TTTAAA). Both *CEN3* and *CEN4* contain three closely spaced *Dra*I sites within their CDEII.

Permeabilized sphearoplasts prepared from cells treated at 38°C were digested with an increasing amount of *Dra*I and DNA was purified after deproteinization. For the analysis of *CEN3*, purified DNA samples were digested with *Bam*HI. If the *Dra*I sites within the *CEN3* CDEII are accessible to the enzyme, *Bam*HI digestion after the deproteinization will give rise to the 480 bp band. As shown in Figure 3C *CEN3*, the 480 bp cutting band appeared in *nps1-105* chromatin lanes but not in wild type ones. The result is consistent with that of the MNase digestion in Figure 3B.

In the case of *CEN4*, two additional *Dra*I sites are located both to the left and right sides flanking the core centromere elements at the distance of 626 and 611 bp, respectively. So, in this case, the accessibility of the *Dra*I sites within CDEII and either or both sites in the flanking region, or the accessibility of the sites only in the flanking region will give rise of a cutting fragment of ~600 or 1237 bp, respectively (Fig. 3C, *CEN4*). Neither 600 nor 1237 bp band was observed with wild type chromatin, indicating the *Dra*I sites in CDEII and at least one site in the flanking region are protected from the digestion. In contrast, in the mutant chromatin lanes, the appearance of 600 bp band is apparent, showing the digestion of *Dra*I sites within CDEII and in the either site in the flanking region. In Figure 3C *CEN4* panel, 2400 and 2100 bp fragment (arrowheads 1 and 2, respectively) appeared in both wild type- and *nps1-105* and *nps1-105* chromatin lanes, respectively. In our analysis, the *Dra*I site flanking the right side of *CEN4* core elements is susceptible to the digestion in both wild type and the mutant chromatin (data not shown). Database searches for *Dra*I cleavage sites in the DNA region neighboring *CEN4* revealed that two additional sites are located at 2423 and 2111 bp upstream of the right-most *Dra*I site in Figure 3C. Therefore, the proximal *Dra*I site is protected from the digestion in the wild type but not in the mutant. The results show that in chromosome IV, at least 1.5 kb DNA region in the left side of the centromere core elements may be assembled in phased nucleosome array and the structural integrity of both centromere core and flanking region are perturbed in *nps1-105* after the treatment at 38°C. With wild type or the mutant cells grown at 27°C, no increase in the sensitivity to *Dra*I was observed at both *CEN3* and *CEN4* DNA (data not shown).

Saunders *et al*. (34) reported that nucleosome depletion alters the chromatin structure of centromeres. A loss of nucleosomes increases more positively supercoiled species in closed circular DNA. To ask if the perturbed structural integrity of centromere chromatin in the *nps1-105* mutant results from the loss of nucleosomes, we analyzed the distribution of topoisomers of naturally occurring yeast 2 μm plasmid. This plasmid exists as a covalently closed circular mini-chromosome assembled into nucleosomal chromatin (reviewed in 35). No change of the topoisomer distribution was introduced by the heat treatment either in wild type or in the mutant, suggesting that the alteration of the centromere structure of the mutant is not a result of the loss of nucleosomes (Fig. 3D).

The *nps1-105* mutation affects transmission fidelity of mini-chromosome

Mutations in *CEN* DNA or histone H4 and depletion of histones H4 or H2B affect the chromatin structure at the centromere and cause chromosome missegregation (36–41). We asked if the *nps1-105* mutation affects chromosome segregation by monitoring the rate of loss (1:0 segregation) and non-disjunction (2:0 segregation) events in *nps1-105/nps1-105 ade2-101/ade2-101* diploid carrying *SUP11* on a mini-chromosome. In this assay, loss and non-disjunction events occurred on the first division after plating result in the appearance of half-pink half-red and half-white half-red colonies, respectively (42,43).

The rates of 1:0 and 2:0 segregation of the wild type cells that were grown at 25°C were both 0.1% and these rates remained unaltered after the 3 h treatment at 38°C. On the other hand, 2:0 segregation rate was noticeably higher in the mutant cells that were grown at 25°C and the rate was increased by the heat treatment (Table 1, experiment 1). The rate of 1:0 segregation in the mutant was somewhat higher than the wild type but was not notably increased by the heat treatment. The results indicating that the *nps1-105* mutation affects the segregation of the plasmid.

We next carried out this assay for the cells treated with TBZ at semipermissive temperature (34°C). Although the rates of 1:0 and 2:0 segregation in the mutant cells were unaltered in the absence of TBZ, the presence of the drug during the 3 h incubation increased the rate of 2:0 segregation (Table 1, experiment 2). The same treatment induced little increase of 2:0 segregation rate in the wild type cells, suggesting that missegregation of mini-chromosome in the mutant is caused by the failure during the reassembly of microtubules.

DISCUSSION

We isolated a temperature-sensitive allele of *NPS1*, *nps1-105*, and found that the mutation causes the alteration of chromatin structure surrounding the centromeric DNA region at elevated temperature. As the centromere chromatin structure is known to be maintained throughout the yeast cell cycle as well (39), this alteration in *nps1-105* seems not to be the result of G2/M arrest of the mutant cells. Therefore, it was suggested that in the *NPS1* mutant, impaired chromatin structure at centromeres may lead to a loss of kinetochore function and the cells arrest at G2/M phase through the spindle-assembly checkpoint system. Several lines of evidence support this idea. First, the *nps1-105* mutant is specifically sensitive to microtubule-destabilizing agents (Fig. 1). It is known that the mutation in the genes encoding kinetochore components causes elevated sensitivity to benomyl (44–47). Second, the *nps1-105* cell-cycle-arrest phenotype is *MAD1* dependent (Fig. 2). Finally, the *nps1-105* mutation causes an increase in the frequency of non-disjunction of mini-chromosome (Table 1). Non-disjunction events are resulted from the segregation of both replicated sister chromatids to the same pole at anaphase. A subset of non-disjunction events are caused by the failure of the centromeres of paired sister chromatids to interact properly with the microtubules.

Table 1. Analysis of *NPS1* function in mitotic chromosome transmission by half-sectored colonies[a]

Strain	Heat treatment (h)	TBZ	Colonies (%) P+W	R	W/P	P/R (1:0)	W/R (2:0)	Total no. of colonies scored
Experiment 1	38°C	60 μg/ml						
WT	0	–	92	7.5	0.1	0.1	0.1	1628
	3	–	87	12.8	0.1	0.2	0.1	1527
nps1-105	0	–	84	14.0	0.9	0.3	0.6	1246
	3	–	82	14.3	1.9	0.4	1.5	2372
Experiment 2	34°C							
WT	0	–	87	12.4	0.1	0.1	0.1	1373
	3	–	86	13.9	0.1	0.0	0.2	1900
	3	+	87	13.8	0.1	0.1	0.3	1141
nps1-105	0	–	86	12.6	0.5	0.1	0.5	1518
	3	–	85	13.2	0.5	0.1	0.7	1995
	3	+	82	13.9	1.9	0.3	1.6	1278

[a]*nps1-105* (YTW-n9D, *a*/α *ade2-101/ade2-101 nps1-105/nps1-105*) and its isogenic wild type (WT) strain (YTW-30D), harboring pHM410 (*CEN4 SUP11 URA*3) were subjected to heat treatment. Cells were removed from the cultures at the indicated times and plated on color media plates. The cells were allowed to form colonies by the incubation at 25°C for 5 days. The percentage of each colony type was calculated and is presented in the table. P, W and R indicate pink, white and red colonies, and W/P, P/R and W/R indicate half-white half-pink, half-pink half-red and half-white half-red sectored colonies, respectively. Standard deviation was within 10%.

To explain the phenotypes of the *nps1-105* mutant, there can be at least three possibilities. The first is that Nps1p plays a direct role on the organization and/or maintenance of the centromere chromatin structure independently from RSC complex. At present, four genes encoding RSC components are identified including *NPS1* (3,21,48). Analysis of the conditional mutant alleles of these genes is required for understanding the role of RSC complex in chromatin structure. The second model is that Nps1p functions through RSC complex as a transcriptional regulator resembling SNF/SWI complex for genes essential for the assembly of certain chromatin structure of centromeres. Previous studies indicate that depletion of histone H2B or H4 alters chromatin structure of centromeres and causes G2 arrest (49–51). Nonetheless, phenotypes reported with the loss of either histones are different from that of *nps1–105* in several points. First, depletion of either histones caused elevated sensitivity to MNase in overall chromatin, while the *nps1-105* mutation did not (Fig. 3A). Second, the reduction of superhelical density in covalently closed circular plasmid was introduced by the loss of either histones but not by the defect of *nps1-105* (Fig. 3D). Finally, the cell cycle arrest by the histone depletion was irreversible: the cells carrying inducible allele of either histone H2B or H4 lost viability upon shift to the repressed conditions within 2 h. On the other hand, the *nps1-105* mutants remained viable at least 8 h in the restrictive condition when the *MAD1* gene is functional (Fig. 2). Accordingly, Nps1p seems not to affect at least the expression of histone genes. A third possibility is that Nps1p acts as a component of RSC complex on the organization or modulation of the centromeric chromatin structure. The yeast centromeric DNA is packed into a unique chromatin structure (30). In addition, the nuclease-protected region within the centromere is highly resistant to ionic conditions that are known to disrupt most loose DNA–protein complexes (52) and is thought to contain specialized nucleosomes. These nucleosomes are suggested to contain Cse4p, a yeast homolog of the human kinetochore protein, CENP-A, in place of histone H3 (53). CENP-A was first identified using sera from patients suffering CREST (calcinosis, Raynaud's phenomenon, esophageal dysmotility, sclerodactyly and telagiectasia) and shown to be a centromere-specific protein which has a domain resembling histone H3 (54). *CSE4* was isolated in a screen for genes that cause an increase in the rate of loss of an artificial chromosome bearing a partial loss of function mutation in CDEII and found to be essential for mitotic growth (55). The phenotypes of temperature-sensitive *CSE4* allele, *cse4-1*, are resemble to those of *nps1-105*: the *cse4-1* mutant arrest with a predominance of large budded cells containing single G2 nuclei and short bipolar mitotic spindles at elevated temperature and shows the increased non-disjunction frequency of a chromosome bearing a mutant centromere DNA sequence (53). Although the yeast centromeric DNA is packed into specialized nucleosomes, the question of how these specialized nucleosomes are properly localized in centromeres is not answered yet. Fundamentally, the binding of histones to DNA is not dependent on specific DNA sequence. In nuclei of growing cells, the amount of conventional nucleosomes may be much more abundant than that of specialized nucleosomes. In case of human cells, targeting of CENP-A to centromeres requires that CENP-A expression is uncoupled from histone H3 synthesis during S phase: CENP-A mRNA accumulates later in the cell cycle than histone H3, peaking in G2 (56). On the other hand, the mRNA of *CSE4* is reported to present at relatively constant levels throughout the cell cycle (53). In addition, whether Cse4p possesses the DNA-binding activity with higher affinity to centromere DNA is obscure. The simplest scenario to explain the role of RSC is that the complex may be required for recruiting specialized nucleosomes, and organizing and/or maintaining the unique chromatin structure in the distinct region of the genome. In this regard, biochemical and genetic properties of *SFH1*, a gene encoding another component of RSC, are of interest (21). A temperature-sensitive *SFH1* mutation, *sfh1-1*, causes G2/M arrest at elevated temperature similar to that of *nps1-105*. The Sfh1 protein is phosphorylated in the G1 phase and dephosphorylated upon progression to the S phase. Because Sfh1p is required for the

progression through G2/M, the phosphorylation of Sfh1p is suggested to negatively regulate Sfh1p function: thus, the protein is likely to be activated by dephosphorylation at the S phase. The organization of newly synthesized DNA properly into highly ordered chromatin structure occurs in tight link with their synthesis during the S phase.

However, our results do not exclude the possibility of requirement of RSC for transcriptional regulation. Cairns *et al*. reported that RSC is at least 10-fold more abundant than SNF/SWI complex (3). Immunofluorescent localization of Nps1p with anti-Nps1p antibody or by expressing Nps1-GFP fusion protein revealed that this protein is not concentrated in the specific region of the nucleus but localized over the entire region stainable with DAPI (1; E.Tsuchiya, unpublished result). The observation indicates that Nps1p or RSC functions not only in the organization of centromere chromatin structure but also in the organization of another chromatin region or in the transcriptional regulation. The analysis on these questions is in progress in our laboratory. It is of interest that two of the *spt* (suppressor of Ty) mutations, *spt4-138* and *spt6-140*, show *ctf* (chromosome transmission fidelity) phenotype and are thought to cause altered chromatin structure at centromeres (57). The *spt* mutants were identified as extragenic suppressors of transcriptional defects caused by Ty or Ty delta element insertions in the 5′ regions of the *HIS4* and *LYS2* genes (58,59). Spt4p, Spt5p and Spt6p function in a complex (60) which can repress transcription (61). There might be several protein complexes required for the organization and/or alteration of the higher order structure of chromatin concerning the progression of cell cycle and the transcriptional regulation.

ACKNOWLEDGEMENTS

We are grateful of our colleagues for helpful discussions and encouragement. We thank H.Matsuzaki and M.Shimizu for providing pHM410 and for technical advice and discussions. This work was supported in part by grant-in-aid 08274214 and 09263211 for scientific research from the Ministry of Education, Science and Culture of Japan.

REFERENCES

1 Tsuchiya,E., Uno,M., Kiguchi,A., Masuoka,K., Kanemori,Y., Okabe,S. and Miyakawa,T. (1992) *EMBO J.*, **11**, 4017–4026.
2 Laurent,B.C., Yang,X. and Carlson,M. (1992) *Mol. Cell. Biol.*, **12**, 1893–1902.
3 Cairns,B.R., Lorch,Y., Li,Y., Zhang,M., Lacomis,L., Erdjument-Bromage,H., Tempst,P., Du,J., Laurent,B.C. and Kornberg,R.D. (1996) *Cell*, **87**, 1249–1260.
4 Winston,F. and Carlson,M. (1992) *Trends Genet.*, **8**, 387–391.
5 Carlson,M. and Laurent,B.C. (1994) *Curr. Opin. Cell Biol.*, **6**, 396–402.
6 Peterson,C.L. and Tamkun,J.W. (1995) *Trends Biochem. Sci.*, **20**, 143–146.
7 Kingston,R.E., Bunker,C.A. and Imbalzano,A.N. (1996) *Genes Dev.*, **10**, 905–920.
8 Pazin,M.J. and Kadonaga,J.T. (1997) *Cell*, **88**, 737–740.
9 Cairns,B.R., Kim,Y.J., Sayre,M.H., Laurent,B.C. and Kornberg,R.D. (1994) *Proc. Natl Acad. Sci. USA*, **91**, 1950–1954.
10 Côté,J., Quinn,J., Workman,J.L. and Peterson,C.L. (1994) *Science*, **265**, 53–60.
11 Peterson,C.L., Dingwall,A. and Scott,M.P. (1994) *Proc. Natl Acad. Sci. USA*, **91**, 2905–2908.
12 Treich,I., Cairns,B.R., Santos,T., Brewster,E. and Carlson,M. (1995) *Mol. Cell. Biol.*, **15**, 4240–4248.
13 Imbalzano,A.N., Kwon,H., Green,M.R. and Kingston,R.E. (1994) *Nature*, **370**, 481–485.
14 Kown,H., Imbalzano,A.N., Khavari,P.A., Kingston,R.E. and Green,M.R. (1994) *Nature*, **370**, 477–481.
15 Wang,W., Côté,J., Xue,Y., Zhou,S., Khavari,P.A., Bigger,S.R., Muchardt,C., Kalpana,G., Goff,S.P., Yaniv,M., Workman,J.L., *et al.* (1996) *EMBO J.*, **15**, 5370–5382.
16 Wang,W., Xue,Y., Zhou,S., Kuo,A., Cairns,B.R., Tijan,R. and Crabtree,G.R. (1996) *Genes Dev.*, **10**, 2117–2130.
17 Tamkun,J.W., Deuring,R., Scott,M.P., Kissinger,M., Pattatucci,A.M., Kaufman,T.C. and Kennison,J.A. (1992) *Cell*, **68**, 561–572.
18 Tsukiyama,T. and Wu,C. (1995) *Cell*, **83**, 1011–1020.
19 Tsukiyama,T., Daniel,C., Tamkun,J. and Wu,C. (1995) *Cell*, **83**, 1021–1030.
20 Laurent,B.C., Treich,I. and Carlson,M. (1993) *Genes Dev.*, **7**, 583–591.
21 Cao,Y., Cairns,B.R., Kornberg,R.D. and Laurent,B.C. (1997) *Mol. Cell. Biol.*, **17**, 3323–3334.
22 Rose,M.D., Winston,F. and Hieter,P. (1990) *Methods in Yeast Genetics*. Cold Spring Harbor Laboratory Press, Cold Spring Harbor, NY.
23 Rothstein,R. (1983) *Methods Enzymol.*, **101**, 202–211.
24 Szent-Gyorgyi,C. and Isenberg,I. (1983) *Nucleic Acids Res.*, **11**, 3717–3736.
25 Veit,B.E. and Fangman,W.L. (1985) *Mol. Cell. Biol.*, **5**, 2190–2196.
26 Ling,X., Harkness,T.A.A., Schultz,M.C., Fisher-Adams,G. and Grunstein,M. (1996) *Genes Dev.*, **10**, 686–699.
27 Saavedra,R.A. and Huberman,J.A. (1986) *Cell*, **45**, 65–70.
28 Koshland,D. and Hieter,P. (1987) *Methods Enzymol.*, **155**, 351–372.
29 Rudner,A.D. and Murray,A.W. (1996) *Curr. Opin. Cell. Biol.*, **8**, 773–780.
30 Bloom,K.S. and Carbon,J. (1982) *Cell*, **29**, 305–317.
31 Clark,L. and Carbon,J. (1980) *Nature*, **287**, 504–509.
32 Fitzgerald-Hayes,M., Clark,M. and Carbon,J. (1982) *Cell*, **29**, 235–244.
33 Hegemann,J.H. and Fleig,U.N. (1993) *Bioessays*, **15**, 451–460.
34 Saunders,M.J., Yeh,E., Grunstein,M. and Bloom,K. (1990) *Mol. Cell. Biol.*, **10**, 5721–5727.
35 Broach,J.R. (1981) In Strathern,J.N., Jones,E.W. and Broach,J.R. (eds), *The Molecular Biology of the Yeast Saccharomyces: Life Cycle and Inheritance*. Cold Spring Harbor Laboratory Press, Cold Spring Harbor, NY, pp. 445–470.
36 Meeks-Wagner,D. and Hartwell,L.H. (1986) *Cell*, **44**, 43–52.
37 Saunders,M. Fitzgerald-Hayes,M. and Bloom,K. (1988) *Proc. Natl Acad. Sci. USA*, **85**, 175–179.
38 Bloom,K., Hill,A., Kenna,M. and Saunders,M. (1989) *Trends Biochem. Sci.*, **14**, 223–227.
39 Saunders,M.I., Yeh,E., Grunstein,M. and Bloom,K. (1990) *Mol. Cell. Biol.*, **10**, 5721–5727.
40 Densmore,L., Payne,W. and Fitzgerald-Hayes,M. (1991) *Mol. Cell. Biol.*, **11**, 154–165.
41 Smith,M.M., Yang,P., Santesteban,M.S., Boon,P.W., Goldstein,A.T. and Megee,P.C. (1996) *Mol. Cell. Biol.*, **16**, 1017–1026.
42 Hieter,P., Mann,C., Snyder,M. and Davis,R.W. (1985)*Cell*, **40**, 381–392.
43 Koshland,D., Kent,J.C. and Hartwell,L.H. (1985) *Cell*, **40**, 393–403.
44 Shero,J.H. and Hieter,P. (1991) *Genes Dev.*, **5**, 549–560.
45 Brown,M.T., Goetsch,L. and Hartwell,L.H. (1993) *J. Cell. Biol.*, **123**, 387–403.
46 Li,Y. and Benezra,R. (1996) *Science*, **274**, 246–248.
47 Wang,Y. and Burke,D.J. (1997) *Mol. Cell. Biol.*, **17**, 620–626.
48 Treich,I. and Carlson,M. (1997) *Mol. Cell. Biol.*, **17**, 1768–1775.
49 Han,M., Chang,M., Kim,U. and Grunstein,M. (1987) *Cell*, **48**, 589–597.
50 Kim,U.J., Han,M., Kayne,P. and Grunstein,M. (1988) *EMBO J.*, **7**, 2211–2219.
51 Morgan,B.A., Mittman,B.A. and Smith,M.M. (1991) *Mol. Cell. Biol.*, **11**, 4111–4120.
52 Bloom,K.S., Amaya,E. and Yeh,E. (1984) *J. Cell Biol.*, **99**, 1559–1568.
53 Stoler,S., Keith,C.K., Curnick,K.E. and Fitzgerald-Hayes,M. (1995) *Genes Dev.*, **9**, 573–586.
54 Palmer,D.K., O'Day,K., Trong,H.L., Charbonneau,H. and Margolis,R.L. (1991) *Proc. Natl Acad. Sci. USA*, **88**, 3734–3738.
55 Xiao,Z., McGrew,J.T., Schroeder,A.J. and Fiztgerald-Hayes,M. (1993) *Mol. Cell. Biol.*, **13**, 4691–4702.
56 Shelby,R.D., Vafa,O. and Sullivan,K.F. (1997) *J. Cell. Biol.*, **136**, 501–513.
57 Basrai,M.A., Kingsbury,J., Koshl,D., Spencer,F. and Hieter,P. (1996) *Mol. Cell. Biol.*, **16**, 2838–2847.
58 Winston,F., Chaleff,D., Valent,B. and Fink,G. (1984) *Genetics*, **107**, 179–197.
59 Fassler,J.S. and Winston,F. (1988) *Genetics*, **118**, 203–212.
60 Swanson,M.S. and Winston,F. (1992) *Genetics*, **132**, 325–336 .
61 Wolffe,A.P. and Pruss,D. (1996) *Curr. Biol.*, **6**, 234–237.